Singapore Management University

Institutional Knowledge at Singapore Management University

Research Collection School Of Computing and Information Systems

School of Computing and Information Systems

6-1994

Production and decay of D1 (2420)0 and D2* (2460)0

AVERY, P.; et al.

M. THULASIDAS

Singapore Management University, manojt@smu.edu.sg

Follow this and additional works at: https://ink.library.smu.edu.sg/sis_research



Part of the Computer Engineering Commons, and the Databases and Information Systems Commons

Citation

This Journal Article is brought to you for free and open access by the School of Computing and Information Systems at Institutional Knowledge at Singapore Management University. It has been accepted for inclusion in Research Collection School Of Computing and Information Systems by an authorized administrator of Institutional Knowledge at Singapore Management University. For more information, please email cherylds@smu.edu.sg.

Production and Decay of D₁ $(2420)^0$ and **D**₂* $(2460)^0$

P. Avery, A. Freyberger, J. Rodriguez, R. Stephens, S. Yang, J. Yelton, D. Cinabro, S. Henderson, T. Liu, M. Saulnier, R. Wilson, H. Yamamoto, T. Bergfeld, 3 B.I. Eisenstein, G. Gollin, B. Ong, M. Palmer, M. Selen, J. J. Thaler, K.W. Edwards, M. Ogg, B. Spaan, A. Bellerive, D.I. Britton, E.R.F. Hyatt, D.B. MacFarlane, P.M. Patel, A.J. Sadoff, R. Ammar, S. Ball, P. Baringer, A. Bean, D. Besson, D. Coppage, N. Copty, R. Davis, N. Hancock, M. Kelly, S. Kotov, I. Kravchenko, N. Kwak, H. Lam, Y. Kubota, M. Lattery, M. Momayezi, J.K. Nelson, S. Patton, D. Perticone, R. Poling, V. Savinov, S. Schrenk, R. Wang, M.S. Alam, ⁹ I.J. Kim, ⁹ B. Nemati, ⁹ J.J. O'Neill, ⁹ H. Severini, ⁹ C.R. Sun, ⁹ M.M. Zoeller, ⁹ G. Crawford, ¹⁰ C. M. Daubenmier, ¹⁰ R. Fulton, ¹⁰ D. Fujino, ¹⁰ K.K. Gan, ¹⁰ K. Honscheid, ¹⁰ H. Kagan, ¹⁰ R. Kass, ¹⁰ J. Lee, ¹⁰ R. Malchow, ¹⁰ Y. Skovpen, ^{10*} M. Sung, ¹⁰ C. White, ¹⁰ F. Butler, ¹¹ X. Fu, ¹¹ G. Kalbfleisch, ¹¹ W.R. Ross, ¹¹ P. Skubic, ¹¹ M. Wood, ¹¹ J.Fast, ¹² R.L. McIlwain, ¹² T. Miao, ¹² D.H. Miller, ¹² M. Modesitt, ¹² D. Payne, ¹² E.I. Shibata, ¹² I.P.J. Shipsey, ¹² P.N. Wang, ¹² M. Battle, ¹³ J. Ernst, ¹³ L. Gibbons, ¹³ Y. Kwon, ¹³ S. Roberts, ¹³ E.H. Thorndike, ¹³ C.H. Wang, ¹³ J. Dominick, ¹⁴ M. Lambrecht, ¹⁴ S. Sanghera, ¹⁴ V. Shelkov, ¹⁴ T. Skwarnicki, ¹⁴ R. Stroynowski, ¹⁴ I. Volobouev, ¹⁴ G. Wei, ¹⁴ P. Zadorozhny, ¹⁴ M. Artuso, ¹⁵ M. Goldberg, ¹⁵ D. He, ¹⁵ N. Horwitz, ¹⁵ R. Kennett, ¹⁵ R. Mountain, ¹⁵ G.C. Moneti, ¹⁵ F. Muheim, ¹⁵ Y. Mukhin, ¹⁵ S. Playfer, ¹⁵ Y. Rozen, ¹⁵ S. Stone, ¹⁵ M. Thulasidas, ¹⁵ G. Vasseur, ¹⁵ X. Xing, ¹⁵ G. Zhu, ¹⁵ J. Bartelt, ¹⁶ S.E. Csorna, ¹⁶ Z. Egyed, ¹⁶ V. Jain, ¹⁶ K. Kinoshita, ¹⁷ B. Barish, ¹⁸ M. Chadha, ¹⁸ S. Chan, ¹⁸ D.F. Cowen, ¹⁸ G. Eigen, ¹⁸ J.S. Miller, ¹⁸ C. O'Grady, ¹⁸ J. Urheim, ¹⁸ A.J. Weinstein, ¹⁸ D. Acosta, ¹⁹ M. Athanas, ¹⁹ G. Masek, ¹⁹ H.P. Paar, ¹⁹ J. Gronberg, ²⁰ R. Kutschke, ²⁰ S. Menary, ²⁰ R.J. Morrison,²⁰ S. Nakanishi,²⁰ H.N. Nelson,²⁰ T.K. Nelson,²⁰ C. Qiao,²⁰ J.D. Richman,²⁰ A. Ryd, ²⁰ H. Tajima, ²⁰ D. Sperka, ²⁰ M.S. Witherell, ²⁰ M. Procario, ²¹ R. Balest, ²² K. Cho,²² M. Daoudi,²² W.T. Ford,²² D.R. Johnson,²² K. Lingel,²² M. Lohner,²² P. Rankin, ²² J.G. Smith, ²² J.P. Alexander, ²³ C. Bebek, ²³ K. Berkelman, ²³ K. Bloom, ²³ T.E. Browder, ^{23†} D.G. Cassel, ²³ H.A. Cho, ²³ D.M. Coffman, ²³ D.S. Crowcroft, ²³ P.S. Drell, ²³ R. Ehrlich, ²³ P. Gaidarev, ²³ M. Garcia-Sciveres, ²³ B. Geiser, ²³ B. Gittelman, ²³ S.W. Gray,²³ D.L. Hartill,²³ B.K. Heltsley,²³ C.D. Jones,²³ S.L. Jones,²³ J. Kandaswamy,²³ N. Katayama, ²³ P.C. Kim, ²³ D.L. Kreinick, ²³ G.S. Ludwig, ²³ J. Masui, ²³ J. Mevissen, ²³ N.B. Mistry, ²³ C.R. Ng, ²³ E. Nordberg, ²³ J.R. Patterson, ²³ D. Peterson, ²³ D. Rilev, ²³ S. Salman,²³ M. Sapper,²³ and F. Würthwein²³

(CLEO Collaboration)

¹ University of Florida, Gainesville, Florida 32611 ²Harvard University, Cambridge, Massachusetts 02138 ³ University of Illinois, Champaign-Urbana, Illinois, 61801 ⁴Carleton University, Ottawa, Ontario K1S 5B6 and the Institute of Particle Physics, Canada ⁵ McGill University, Montréal, Québec H3A 2T8 and the Institute of Particle Physics, Canada ⁶ Ithaca College, Ithaca, New York 14850 ⁷ University of Kansas, Lawrence, Kansas 66045 ⁸ University of Minnesota, Minneapolis, Minnesota 55455 ⁹ State University of New York at Albany, Albany, New York 12222 ¹⁰ Ohio State University, Columbus, Ohio, 43210 ¹¹University of Oklahoma, Norman, Oklahoma 73019 ¹²Purdue University, West Lafayette, Indiana 47907 ¹³ University of Rochester, Rochester, New York 14627 ¹⁴Southern Methodist University, Dallas, Texas 75275 ¹⁵Syracuse University, Syracuse, New York 13244 ¹⁶ Vanderbilt University, Nashville, Tennessee 37235 ¹⁷ Virginia Polytechnic Institute and State University, Blacksburg, Virginia, 24061 ¹⁸ California Institute of Technology, Pasadena, California 91125 ¹⁹ University of California, San Diego, La Jolla, California 92093 ²⁰ University of California, Santa Barbara, California 93106 ²¹Carnegie-Mellon University, Pittsburgh, Pennsylvania 15213 ²² University of Colorado, Boulder, Colorado 80309-0390 ²³Cornell University, Ithaca, New York 14853

Abstract

We have investigated $D^+\pi^-$ and $D^{*+}\pi^-$ final states and observed the two established L=1 charmed mesons, the $D_1(2420)^0$ with mass 2421^{+1+2}_{-2-2} MeV/c² and width 20^{+6+3}_{-5-3} MeV/c² and the $D_2^*(2460)^0$ with mass $2465\pm 3\pm 3$ MeV/c² and width 28^{+8+6}_{-7-6} MeV/c². Properties of these final states, including their decay angular distributions and spin-parity assignments, have been studied. We identify these two mesons as the $j_{light}=3/2$ doublet predicted by HQET. We also obtain constraints on $\Gamma_S/(\Gamma_S+\Gamma_D)$ as a function of the cosine of the relative phase of the two amplitudes in the $D_1(2420)^0$ decay.

*Permanent address: INP, Novosibirsk, Russia

[†]Permanent address: University of Hawaii at Manoa

I. INTRODUCTION

Heavy Quark Effective Theory (HQET) predicts the presence of an approximate flavorspin symmetry for hadrons containing one heavy quark $(m_Q \gg \Lambda_{QCD})$ [1,2]. One of the outstanding issues in this theory is whether the charm quark is sufficiently heavy for the approximations made in the theory to be valid. One testable prediction of HQET is the partial wave structure of the decays of the D_J mesons. The D_J mesons consist of one charmed quark (Q) and one light quark (\overline{q}) with relative orbital angular momentum L. When L=1, there are four states with spin-parity $J^P=0^+, 1^+, 1^+$ and 2^+ . In the notation introduced by the Particle Data Group [3], these states are labeled D_0^* , D_1 for both 1^+ states, and D_2^* , respectively.

Parity and angular momentum conservation place restrictions on the strong decays of these D_J states to $D\pi$ and $D^*\pi$: the 0^+ state can decay only to $D\pi$ through S-wave decay, either 1^+ state can decay to $D^*\pi$ through S-wave or D-wave decays, and the 2^+ state can decay to both $D\pi$ and $D^*\pi$ only through D-wave decays.

In the decay $D_J \to D^*\pi$, the helicity angular distribution of the D^* can be used to analyze the spin of the parent D_J . The helicity angle, denoted by α , is defined as the angle between the π^- from the decay $D_J^0 \to D^{*+}\pi^-$ and the π^+ from the decay $D^{*+} \to D^0\pi^+$, both measured in the D^{*+} rest frame. Regardless of the initial polarization of the D_J states, the predicted helicity angular distributions are:

$$\frac{d N}{d \cos \alpha} \propto \begin{cases} \sin^2 \alpha & (2^+ \text{ state}) \\ 1 & (\text{pure S-wave } 1^+ \text{ state}) \\ 1 + 3\cos^2 \alpha & (\text{pure D-wave } 1^+ \text{ state}) \end{cases}$$
(1)

Two D_J^0 states have been observed previously [4–8]. However, the decay angular analyses performed were all incomplete and not in total agreement with each other.

In the limit $m_Q \to \infty$, the mesons are described by $j = S_q + L$ (total angular momentum of the light quark). When m_Q is large, but not infinite, the properties of the mesons will also depend on S_Q (spin of the heavy quark) and $J = j + S_Q$ (total angular momentum). The mesons with L = 1 are then labeled as:

$$L_J^{(j)P} = \begin{cases} P_0^{(1/2)+}, & P_1^{(1/2)+} \\ P_1^{(3/2)+}, & P_2^{(3/2)+} \end{cases} & (j = 1/2 \ doublet) \\ (j = 3/2 \ doublet) \end{cases}$$
(2)

The j=1/2 mesons are predicted to decay exclusively in an S-wave, while the j=3/2 mesons decay only in a D-wave [1,9]. Mesons which decay via a D-wave are predicted to be relatively narrow (widths of tens of MeV/c²), while those of the other doublet are predicted to be quite broad (hundreds of MeV/c²). The $P_2^{(3/2)+}$ state can decay to both $D\pi$ and $D^*\pi$. Models [9–11] predict the ratio of the branching fractions, $B(D_2^* \to D\pi)/B(D_2^* \to D^*\pi)$, to lie in the range from 1.5 to 3.0.

Because the mass of the charmed quark is not infinite, the $P_1^{(3/2)+} \to D^*\pi$ decay can also proceed via an S-wave. HQET predicts that this S-wave amplitude is small compared with typical S-wave amplitudes, but makes no prediction for the relative magnitudes of the S-wave and D-wave amplitudes for this decay. However, particular models do make such predictions [10,11].

The large data sample collected with the CLEO II detector allows us to identify clearly two of the D_J^0 states, to measure their corresponding angular distributions and to test some of the HQET predictions.

II. DATA SAMPLE AND EVENT SELECTION

The data used in this analysis were selected from hadronic events produced in e^+e^- annihilations at CESR and collected with the CLEO II detector. Both neutral and charged particles are measured with excellent resolution and efficiency by the CLEO II detector. A detailed description of the detector can be found elsewhere [12]. The center-of-mass energies used in this analysis were at the mass of the $\Upsilon(4S)$, $E_{C.M.}=10.580$ GeV, and in the nearby continuum. The data corresponds to an integrated luminosity of 1.7 fb⁻¹.

We selected events that have a minimum of three charged tracks, a total visible energy greater than 15% of the center-of-mass energy (this reduced contamination from two-photon interactions and beam-gas events), and a primary vertex within ± 5 cm in the z-direction and ± 2 cm in the r- ϕ plane of the nominal collision point. All charged tracks were required to have dE/dx information. If available, time-of-flight information was also used.

When reconstructing π^0 candidates, we used pairs of photons from the barrel region with $|\cos\theta| < 0.707$, where the energy resolution is best. The photons were required to have a minimum energy of 50 MeV and to be isolated from charged tracks. All π^0 candidates, whose invariant mass was within 50 MeV/c² of the π^0 mass, were kinematically fit to the known π^0 mass and were required to have a minimum momentum of 65 MeV/c.

III.
$$D_2^{*0} \to D^+\pi^-$$

To reconstruct $D_2^{*0} \to D^+\pi^-$, we first reconstructed the D^+ in the decay mode $K^-\pi^+\pi^+$. We required that the decay angle θ_K , the angle between the direction of the D^+ momentum in the lab and the direction of the K^- momentum in the D^+ rest frame, satisfy the condition $\cos\theta_K < 0.8$, since the background peaks near 1. Each D^+ candidate was then combined with each remaining π^- in the event. In order to reduce combinatorial background we applied the cuts of $x_p(D_2^{*0}) = p(D_2^{*0})/\sqrt{E_{beam}^2 - M(D_2^{*0})^2} > 0.65$ and $\cos\theta_\pi > -0.8$, where the decay angle, θ_π , is defined as the angle between the direction of the D_2^{*0} momentum in the lab and the direction of the π^- momentum in the D_2^{*0} rest frame. We then calculated the total probability, P_{tot} , of the candidate using the particle identification (dE/dx and time-of-flight) and the reconstructed D^+ mass. $P_{tot}(\chi_{tot}^2, N_{dof})$ is defined as the probability to observe $\chi^2 > \chi_{tot}^2$ for N_{dof} degrees of freedom. The data sample is highly contaminated due to the small D^+ signal to background ratio, and this produces a large and broad peaking in the P_{tot} distribution at $P_{tot} = 0$. For the signal this distribution is expected to be flat. We accordingly required $P_{tot} > 0.4$.

[‡]References in this paper to a specific state or decay will always imply that the charge-conjugate state or decay has been included as well.

The spectrum of the mass-difference, $M(D^+\pi^-)-M(D^+)$, for all $D^+\pi^-$ combinations surviving the above cuts is shown in Fig. 1. This spectrum was fitted with a third-order Chebychev polynomial for the background and a Breit-Wigner resonance shape, convoluted with a Gaussian resolution function, for the signal. The σ of this Gaussian function was fixed to 4.5 MeV/c², as determined from Monte Carlo studies. The region from 380 to 430 MeV/c² was excluded from the fit because this region is populated by feed-down, caused by not reconstructing neutrals in the decay chain, $D_J^0 \to D^{*+}\pi^-$, with $D^{*+} \to D^+\pi^0$ or $D^+\gamma$. Our fit yielded 486^{+103}_{-119} signal events with a value $M(D_2^{*0}) - M(D^+) = 596 \pm 3 \pm 3$ MeV/c², which corresponds to a D_2^{*0} mass of $2465 \pm 3 \pm 3$ MeV/c², and an intrinsic width $\Gamma = 28^{+8+6}_{-7-6}$ MeV/c². The second error is systematic and was estimated by varying the cuts, the background parameterization, and the spin of the Breit-Wigner distribution used. Our results for the mass and width of this state, along with previous measurements, are listed in Table I.

IV.
$$D_J^0 o D^{*+}\pi^-$$

To reconstruct $D_J^0 \to D^{*+}\pi^-$ we first reconstructed D^0 's in the decay modes $K^-\pi^+$, $K^-\pi^+\pi^0$, and $K^-\pi^+\pi^+\pi^-$. The D^{*+} candidates were reconstructed by combining each D^0 candidate with each remaining π^+ in the event. Each D^{*+} candidate was then combined with each remaining π^- in the event. In order to reduce combinatorial background, a cut of $x_p(D_J^0) > 0.6$ and a cut of $\cos\theta_\pi > -0.7$ were applied. We calculated P_{tot} using the particle identification (dE/dx and time-of-flight), the D^0 mass, the π^0 mass, and the mass-difference $M(D^{*+}) - M(D^0)$. A purifying cut of $P_{tot} > 0.05$ was then imposed.

The expected angular distributions, outlined previously, can be used to separate the two D_J^0 states decaying to $D^{*+}\pi^-$. In order to resolve the D_1^0 state and improve the signal to background ratio, the D_2^{*0} state was suppressed by requiring $|\cos \alpha| > 0.8$. The $M(D^{*+}\pi^-)$ $M(D^{*+})$ spectrum for all combinations passing the above cuts is shown in Fig. 2(a). The prominent peak observed is due to the D_1^0 state and the shoulder at higher mass is due to the D_2^{*0} state. This spectrum was fitted with a fourth-order Chebychev polynomial for the background and two Breit-Wigner resonance shapes convoluted with Gaussian resolution functions for the signals. The σ 's of these Gaussian functions were fixed to 4.0 MeV/c², as determined from Monte Carlo studies. The mass and width of the higher mass convoluted Breit-Wigner were constrained to the measured values obtained above from the decay $D_2^{*0} \rightarrow$ $D^+\pi^-$, while the parameters of the other convoluted Breit-Wigner were left free. For the suppressed D_2^{*0} state, we obtained 48 ± 30 signal events. For the D_1^0 state, the fit yields 286^{+51}_{-46} signal events, $M(D_1^0)-M(D^{*+})=411^{+1+2}_{-2-2}$ MeV/c², and $\Gamma=20^{+6+3}_{-5-3}$ MeV/c². The measured mass-difference corresponds to a D_1^0 mass of 2421^{+1+2}_{-2-2} MeV/c². The second error is systematic and was estimated by varying the cuts, the mass and width of the fixed state, the background parameterization, and the spin of the Breit-Wigner shapes used to describe the signals. Our results for the mass and width of this state, along with previous measurements, are listed in Table II.

The spectrum of the mass-difference, $M(D^{*+}\pi^{-}) - M(D^{*+})$, with no cut on the helicity angle is shown in Fig. 2(b). A fit to the mass-difference distribution with no helicity angle cut yielded $M(D_1^0) - M(D^{*+}) = 412 \pm 1 \text{ MeV/c}^2$ and $\Gamma = 24^{+5}_{-4} \text{ MeV/c}^2$ in excellent agreement with those obtained above.

V. FRAGMENTATION

The momentum spectra of $D_2^*(2460)^0 \to D^+\pi^-$ and of $D_1(2420)^0 \to D^{*+}\pi^-$ were also obtained by fitting the observed mass-difference distribution in five x_p bins from 0.5 to 1. Fitting the Peterson fragmentation function [13]:

$$\frac{dN}{dx_p} \propto \frac{1}{x_p \left[1 - \frac{1}{x_p} - \frac{\epsilon_p}{1 - x_p}\right]^2} \tag{3}$$

to the acceptance-corrected momentum spectra, shown in Fig. 3(a) and (b), we find $\epsilon_p = 0.034^{+0.018+0.005}_{-0.011-0.005}$ and $0.015^{+0.004+0.001}_{-0.003-0.001}$, respectively, for the $D_2^*(2460)^0$ and the $D_1(2420)^0$. The systematic error was estimated by varying the number and size of the x_p bins used, and by varying the mass and the width of the D_J^0 states. Both spectra are quite hard compared with those observed for continuum production of D and D^* mesons at these center of mass energies [14,15].

VI. CROSS SECTIONS AND PRODUCTION RATIOS

As will be discussed below, measurements of the production rates for the D_J^0 states are, in general, sensitive to the D_J^0 alignment, which is uncertain. When the detector acceptance is flat in $\cos \theta_{\pi}$, the dependence on the alignment can be removed either by including events from the full range of $\cos \theta_{\pi}$ or by selecting events with $\cos \theta_{\pi} > 0$. Monte Carlo studies showed that the efficiency for reconstructing $D_2^*(2460)^0 \to D^+\pi^-$ does not vary over the range $-1 \le \cos \theta_{\pi} \le +1$, while that of $D_J^0 \to D^{*+}\pi^-$ does not vary significantly over the range $\cos \theta_{\pi} > 0$. We accordingly removed the $\cos \theta_{\pi}$ cut for the decay of $D_2^*(2460)^0 \to D^+\pi^-$ and required $\cos \theta_{\pi} > 0$ for the decays of $D_J^0 \to D^{*+}\pi^-$. The measured yields for the decay modes $D_2^*(2460)^0 \to D^+\pi^-$, $D_2^*(2460)^0 \to D^{*+}\pi^-$, and $D_1(2420)^0 \to D^{*+}\pi^-$ were then determined to be 513 ± 81 , 164 ± 41 , and 536 ± 43 signal events, respectively. Using the fragmentation functions to extrapolate to zero momentum, and after correcting for the efficiencies and the relevant D^0 , D^+ , and D^{*+} branching ratios, we have extracted the production cross sections times the branching ratios for $x_p \ge 0$:

$$\sigma(e^+e^- \to D_J^0 X) \cdot B(D_J^0). \tag{4}$$

Our measurements, as well as those of ARGUS [4,5], are summarized in Table III. In these calculations we have used the new CLEO II [16] measurements of the D^{*+} branching ratios. In making comparisons with previous measurements, we scaled the old numbers to compensate for the increase of the $B(D^{*+} \to D^0\pi^+)$. The systematic errors include the uncertainties in the yields of the D_J^0 states, the uncertainties in the branching ratios, and the uncertainty in the extrapolation to $x_p = 0$.

We also extracted the production ratios:

$$N(D_J^0 \to D^+\pi^-)_{x_p>0.6} / N(D^+)_{x_p>0.6}$$
 (5)

and

$$N(D_J^0 \to D^{*+}\pi^-)_{x_p>0.6} / N(D^{*+})_{x_p>0.6}.$$
 (6)

Our measurements, as well as those of ARGUS [4] and CLEO 1.5 [7], are summarized in Table IV.

We then determined the ratio of the branching fractions of the $D_2^*(2460)^0$ state:

$$\frac{B[D_2^*(2460)^0 \to D^+\pi^-]}{B[D_2^*(2460)^0 \to D^{*+}\pi^-]} = 2.2 \pm 0.7 \pm 0.6.$$
 (7)

ARGUS [5] and CLEO 1.5 [7] have measured this quantity to be $3.7 \pm 1.4 \pm 1.9$ and 2.8 ± 1.0 , respectively. Our new result agrees well with the HQET predictions discussed previously.

VII. HELICITY ANGULAR DISTRIBUTIONS

The various spin-parity hypotheses and the corresponding helicity angle distributions, for the general case of decays to $D^*\pi$, are listed in Table V.

A study of the helicity angular distribution, $\cos \alpha$, lends support to the identification of these states as members of the j=3/2 doublet. To study the helicity angle distributions of $D_2^*(2460)^0 \to D^{*+}\pi^-$ and $D_1(2420)^0 \to D^{*+}\pi^-$, we fitted the $M(D^{*+}\pi^-) - M(D^{*+})$ mass-difference spectra in five bins of $\cos \alpha$ from -1 to +1. The masses and widths of both states were fixed to our measured values given above.

In the decay of the $D_2^*(2460)^0$, the D^{*+} and the π^- are emitted in a relative D-wave. This requires the D^{*+} to have a helicity of ± 1 . Thus the form of the helicity angular distribution for the $D_2^*(2460)^0$ state will be $\sin^2 \alpha$, independent of the initial alignment of this state. Monte Carlo studies showed that our efficiency does not vary significantly over the helicity angle. The number of $D_2^*(2460)^0$ events obtained in each $\cos \alpha$ bin is shown in Fig. 4(a).

The general form for the joint decay angular distribution for the $D_1(2420)^0 \rightarrow D^{*+}\pi^-$ is given below, Eq. (8). When the detector acceptance is flat in $\cos \theta_{\pi}$, integration over $\cos \theta_{\pi}$ in either the range $-1 \le \cos \theta_{\pi} \le +1$, or in the range $\cos \theta_{\pi} > 0$, will remove dependence of the $D_1(2420)^0$ helicity angular distribution on the alignment of the $D_1(2420)^0$ state. Monte Carlo studies showed that, in the $\cos \theta_{\pi} > 0$ range, our efficiency does not vary significantly over the plane of the helicity angle and the decay angle. The only case where the efficiency is a little lower, by $\approx 10\%$, is when $\cos \alpha$ is backward and $\cos \theta_{\pi}$ is forward. In this case, the momentum of the slow π^+ in the decay $D^{*+} \rightarrow D^0 \pi^+$ has its minimum value. We thus required $\cos \theta_{\pi} > 0$ and corrected for the relative efficiency of the point at $\cos \alpha < -0.6$, and included the uncertainty in the alignment of the $D_1(2420)^0$ state in the systematic error of the efficiency correction. This yielded the number of $D_1(2420)^0$ events in each $\cos \alpha$ bin as shown in Fig. 4(b). In addition to the statistical errors, the error bars include systematic errors due to the uncertainties in the yields and due to the efficiency correction for the point at $\cos \alpha < -0.6$.

We evaluated the χ^2 per degree of freedom, χ^2/N_{dof} , and confidence level for various hypotheses for the shape of these distributions. The results are listed in Table VI. For the $D_2^*(2460)^0$ state the $\sin^2 \alpha$ hypothesis is preferred, although the isotropic hypothesis is also acceptable. For the $D_1(2420)^0$ state, the $\cos^2 \alpha$ hypothesis is excluded for the first time, at more than 99% CL. This excludes an alternative interpretation of this state as a radial excitation of the D^0 with $J^P = 0^-$. Because the $\sin^2 \alpha$ hypothesis is also excluded, the $\cos \alpha$ distribution, alone, restricts the $D_1(2420)^0$ state to the quantum numbers $J^P = 1^+, 2^-, 3^+ \dots$

Since it is difficult to produce L > 1 in the fragmentation process, $J^P = 1^+$ is the preferred assignment. Because the $D_1(2420)^0$ width is relatively small, this state is identified as the $P_1^{(3/2)+}$ and the $D_2^*(2460)^0$ as its doublet partner, the $P_2^{(3/2)+}$.

To compare with previous results, we also fit the distribution for the $D_2^*(2460)^0$ decay to the form, $A(1 + B\cos^2\alpha)$, which gave the result, $B = -0.74^{+0.49}_{-0.38}$ with $\chi^2/N_{dof} = 0.6/3$ and a CL = 90.6%. Fitting the distribution for the $D_1(2420)^0$ to the same functional form gave the result, $B = 2.74^{+1.40}_{-0.93}$ with $\chi^2/N_{dof} = 2.2/3$ and a CL = 53.2%.

Assuming that the $D_1(2420)^0$ does indeed have $J^P = 1^+$, both S and D wave amplitudes are allowed in its decay to $D^{*+}\pi^-$. The general form of the $D_1(2420)^0 \to D^{*+}\pi^-$ angular distribution is then:

$$\frac{dN}{d\cos\alpha \ d\cos\theta_{\pi}} \propto \frac{\sin^{2}\alpha}{8} \left[(1+\cos^{2}\theta_{\pi}) + \rho_{00}(1-3\cos^{2}\theta_{\pi}) \right] \left\{ 2\Gamma_{S} + \Gamma_{D} + 2\sqrt{2\Gamma_{S}\Gamma_{D}}\cos\varphi \right\} \\
+ \frac{\cos^{2}\alpha}{2} \left[(1-\cos^{2}\theta_{\pi}) - \rho_{00}(1-3\cos^{2}\theta_{\pi}) \right] \left\{ \Gamma_{S} + 2\Gamma_{D} - 2\sqrt{2\Gamma_{S}\Gamma_{D}}\cos\varphi \right\}, \quad (8)$$

where α is the helicity angle, θ_{π} is the decay angle, Γ_{S} is the S-wave partial width, Γ_{D} is the D-wave partial width, φ is the relative phase of the two amplitudes, and ρ_{00} is the fraction of $D_{1}(2420)^{0}$ with helicity 0 in the lab frame. Integrating over $\cos \theta_{\pi}$ from -1 to +1, or from 0 to +1, gives:

$$\frac{1}{N}\frac{dN}{d\cos\alpha} = \frac{1}{2}\left\{\mathbf{R} + (1-\mathbf{R})\left[\frac{1+3\cos^2\alpha}{2}\right] + \sqrt{2\mathbf{R}(1-\mathbf{R})}\cos\varphi\left[1-3\cos^2\alpha\right]\right\}, \tag{9}$$

where $R=\Gamma_S/(\Gamma_S+\Gamma_D)$. Had we not released the $\cos\theta_\pi$ cut or applied a $\cos\theta_\pi>0$ cut, the helicity angle distribution would also have depended on the alignment of the initial state. Previous analyses [5,7,8] did not remove this cut. Once R and $\cos\varphi$ are specified, the shape of the expected $\cos\alpha$ distribution is fixed, and one can then determine the χ^2 that the distribution fits the data points in Fig. 4(b). The shaded region in Fig. 5 shows the region of the R- $\cos\varphi$ plane which is allowed at the 90% CL. The allowed regions fall into two categories. First, if R is small then all values of $\cos\varphi$ are allowed. Second, if $\cos\varphi$ is negative, then a large S-wave partial width is allowed. This can result from mixing between the two 1⁺ states and it may explain the difference between the measured value of the ratio $\Gamma(D_2^{*0})/\Gamma(D_1^0) \sim 1$, and the HQET [2,11] prediction ~ 3 .

VIII. CONCLUSIONS

In conclusion, we have observed the two charmed mesons of masses $2465 \pm 3 \pm 3$ and 2421^{+1+2}_{-2-2} MeV/c², and of widths 28^{+8+6}_{-7-6} and 20^{+6+3}_{-5-3} MeV/c², respectively. The observed helicity angular distributions are in good agreement with expectations for the L=1 c \overline{u} $D_2^*(2460)^0$ and $D_1(2420)^0$ states. We have made the first measurement of $\Gamma_S/(\Gamma_S + \Gamma_D)$ as a function of the relative phase of S and D wave amplitudes in the $D_1(2420)^0 \rightarrow D^{*+}\pi^-$ decay. In addition, the measured widths of both states are relatively narrow, consistent with the predictions for D-wave decays of these states. We have also determined the ratio of the branching fractions of the two decay modes of $D_2^*(2460)^0$ into $D^+\pi^-$ and $D^{*+}\pi^-$, obtaining a value of $2.2 \pm 0.7 \pm 0.6$ which is consistent with the expectation from HQET. Taken together, these results constitute strong evidence for identifying these two D_J^0 states as the $P_2^{(3/2)+}$ and $P_1^{(3/2)+}$ (j=3/2) doublet predicted by HQET.

ACKNOWLEDGMENTS

We gratefully acknowledge the effort of the CESR staff in providing us with excellent luminosity and running conditions. J.P.A. and P.S.D. thank the PYI program of the NSF, I.P.J.S. thanks the YI program of the NSF, G.E. thanks the Heisenberg Foundation, K.K.G., I.P.J.S., and T.S. thank the TNRLC, K.K.G., H.N.N., J.D.R., T.S. and H.Y. thank the OJI program of DOE and P.R. thanks the A.P. Sloan Foundation for support. This work was supported by the National Science Foundation and the U.S. Dept. of Energy.

REFERENCES

- [1] N. Isgur and M.B. Wise, Phys. Rev. Lett. 66, 1130 (1991).
- [2] M. Lu, M. Wise and N. Isgur, Phys. Rev. D 45, 1553 (1992).
- [3] Particle Data Group, K. Hikasa et al., Phys. Rev. D 45, (1992).
- [4] ARGUS Collab., H. Albrecht et al., Phys. Lett. B 221, 422 (1989).
- [5] ARGUS Collab., H. Albrecht et al., Phys. Lett. B 232, 398 (1989).
- [6] E691 Collab., J. C. Anjos et al., Phys. Rev. Lett. 62, 1717 (1989).
- [7] CLEO Collab., P. Avery et al., Phys. Rev. D 41, 774 (1990).
- [8] E687 Collab., P. L. Frabetti et al., Phys. Rev. Lett. 72, 324 (1994).
- [9] J. L. Rosner, Comm. Nucl. Part. Phys. 16, 109 (1986).
- [10] S. Godfrey and R. Kokoski, Phys. Rev. D 43, 1679 (1991).
- [11] A. F. Falk and M. E. Peskin, SLAC-PUB-6311 (1993).
- [12] CLEO Collab., Y. Kubota et al., Nucl. Inst. Meth. A320, 66 (1992).
- [13] C. Peterson et al., Phys. Rev. D 27, 105 (1983).
- [14] ARGUS Collab., H. Albrecht et al., Phys. Lett. B 150, 235 (1985).
- [15] CLEO Collab., D. Bortoletto et al., Phys. Rev. D 37, 774 (1988).
- [16] CLEO Collab., F. Butler at al., Phys. Rev. Lett. 69, 2041 (1992).

TABLES

TABLE I. $D_2^*(2460)^0$ mass and width.

Experiment	$ m Mass~(MeV/c^2)$	Width (MeV/c^2)
CLEO II	$2465 \pm 3 \pm 3$	28^{+8+6}_{-7-6}
CLEO 1.5	$2461 \pm 3 \pm 1$	20^{+9+9}_{-12-10}
ARGUS	$2455 \pm 3 \pm 5$	15^{+13+5}_{-10-10}
E691	$2459 \pm 3 \pm 2$	$20\pm10\pm5$
E687	$2453 \pm 3 \pm 2$	$25\pm10\pm5$

TABLE II. $D_1(2420)^{\rm 0}$ mass and width.

Experiment	$ m Mass~(MeV/c^2)$	$\frac{1}{\text{Width } (\text{MeV/c}^2)}$
CLEO II	2421^{+1+2}_{-2-2}	20^{+6+3}_{-5-3}
CLEO 1.5	$2428 \pm 3 \pm 2$	23^{+8+10}_{-6-4}
ARGUS	$2414 \pm 2 \pm 5$	13^{+6+10}_{-6-5}
E691	$2428 \pm 8 \pm 5$	$58 \pm 14 \pm 10$
E687	$2422 \pm 2 \pm 2$	$15 \pm 8 \pm 4$

TABLE III. Summary of D_J^0 cross sections times branching ratios: $\sigma(e^+e^- \to D_J^0 X) \cdot B(D_J^0)$.

Decay Mode	CLEO II (pb)	ARGUS (pb)
$D_2^*(2460)^0 o D^+\pi^-$	$21.4 \pm 3.4 \pm 4.2$	$68 \pm 21 \pm 28$
$D_2^*(2460)^0 o D^{*+}\pi^-$	$9.5 \pm 2.4 \pm 1.8$	$19 \pm 4 \pm 6$
$D_1(2420)^0 \to D^{*+}\pi^-$	$28.5 \pm 2.3 \pm 3.6$	$32 \pm 4 \pm 9$

TABLE IV. Summary of D_J^0 production ratios: $N(D_J^0 \to D^{(*)+}\pi^-)_{x_p>0.6} / N(D^{(*)+})_{x_p>0.6}$.

Decay Mode	CLEO II (%)	CLEO 1.5 (%)	ARGUS (%)
$D_2^*(2460)^0 \to D^+\pi^-$	$4.7 \pm 0.7 \pm 0.7$	10^{+2+2}_{-2-1}	11^{+4+5}_{-4-5}
$D_2^*(2460)^0 o D^{*+}\pi^-$	$2.1 \pm 0.5 \pm 0.4$	$3.6^{+1.0+0.4}_{-1.0-0.8}$	
$D_1(2420)^0 \to D^{*+}\pi^-$	$6.8 \pm 0.6 \pm 0.9$	$8.9^{+1.1+0.5}_{-1.1-0.5}$	

TABLE V. List of spin-parity hypotheses and the corresponding helicity angle distributions. $A_{\lambda 0}$ is the amplitude to produce D^* with helicity λ .

Spin-Parity Hypothesis	Angular Distribution
0+	forbidden
0-	$\cos^2 lpha$
$1^-, 2^+, 3^-, \dots$	$\sin^2 lpha$
$1^+, 2^-, 3^+, \dots$	$ A_{10} ^2 \sin^2 \alpha + A_{00} ^2 \cos^2 \alpha$

TABLE VI. χ^2 and CL for various angular distributions.

State	Angular Distribution	χ^2/N_{dof}	$\overline{\mathrm{CL}}$
$\overline{D_2^*(2460)^0}$	$\sin^2 \alpha$	1.2/4	87.8%
	isotropic	2.5/4	64.5%
$D_1(2420)^0$	$1+3\cos^2\alpha$	2.3/4	68.1%
	${\rm isotropic}$	23.9/4	83.6×10^{-6}
	$\cos^2 lpha$	28.2/4	11.4×10^{-6}
	$\sin^2 lpha$	93.2/4	27.5×10^{-20}

FIG. 1. The $M(D^+\pi^-)-M(D^+)$ mass-difference distribution.

FIG. 2. The $M(D^{*+}\pi^-)-M(D^{*+})$ mass-difference distribution for (a) $|\cos\alpha|\geq 0.8$ and (b) $-1\leq\cos\alpha\leq+1$.

FIG. 3. The momentum spectra of (a) $D_2^*(2460)^0 \to D^+\pi^-$ and (b) $D_1(2420)^0 \to D^{*+}\pi^-$.

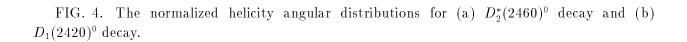


FIG. 5. Plot of $R = \Gamma_S/(\Gamma_S + \Gamma_D)$ versus cosine of the relative phase of S and D wave amplitudes in the $D_1(2420)^0$ decay. The shaded area represents the 90% confidence level allowed region.